Savita Bansal, *Satya Bir Singh*[*]

INVESTIGATION OF CREEP IN ANISOTROPIC CYLINDER USING PLANE STRESS CONDITION

ISTRAŽIVANJE PUZANJA ANIZOTROPNOG CILINDRA U USLOVIMA RAVNOG STANJA NAPONA

Originalni naučni rad / Original scientific paper
Rad primljen / Paper received: 22.09.2024
https://doi.org/10.69644/ivk-2025-01-0106

Adresa autora / Author's address:
Punjabi University, Patiala, Punjab, India
S. Bansal https://orcid.org/0000-0002-0665-3198
S.B. Singh https://orcid.org/0000-0003-1381-4903
[*]email: sbsingh69@yahoo.com

Keywords
- cylinder
- anisotropic material
- constant pressure
- creep analysis
- plane stress

Ključne reči
- cilindar
- anizotropni materijal
- konstatan pritisak
- analiza puzanja
- ravno stanje napona

Abstract

Creep response is investigated in an anisotropic cylinder under plane stress condition using constitutive equations of anisotropic creep theory and Sherby's law, on a thick-walled cylinder of orthotropic material under constant internal pressure. Radial and tangential stress distribution in the cylinder have been calculated and compared for two different cases of anisotropy with that of an isotropic material. It is concluded that anisotropy leads to nominal variation in stress distribution in the thick-walled cylinder under plane stress condition. The study, however, reveals that under plane stress condition, isotropic materials show lesser creep response than anisotropic material and are found to be better from the engineering design point of view.

Izvod

U radu se istražuje puzanje anizotropnog cilindra u uslovima ravnog stanja napona, primenom konstitutivnih jednačina anizotropne teorije puzanja i Šerbijevog zakona, primenjeno na debelozidom cilindru od ortotropnog materijala pod dejstvom konstantnog unutrašnjeg pritiska. Izvedena je raspodela radijalnog i tangencijalnog napona u cilindru i upoređena za dva slučaja anizotropije za izotropan materijal. Zaključuje se da anizotropija dovodi do nominalne varijacije u raspodeli napona kod debelozidog cilindra u uslovima ravnog stanja napona. Međutim, u radu se pokazuje da, u uslovima ravnog stanja napona, izotropni materijali pokazuju manje izraženo puzanje u odnosu na anizotropni materijal i imaju bolja svojstva sa inženjerskog stanovišta.

INTRODUCTION

In modern engineering tools and equipment, cylinders are among the most prevalent shapes of components. New innovations used in nuclear reactors, the space industry, civic, and military applications make extensive use of thick-walled cylinders. Because of the highly pressurised gases and fluids that are transported in cylinders, they become vulnerable to extreme thermomechanical stress which could shorten their service life due to creep. From the viewpoint of assessing the tools and equipment safety, it is important to study creep in various engineering structures having different pressure and temperature conditions.

Many authors have examined thick-walled cylinder creep-related issues in great detail. Wahl et al. /15/ and Rimrott et al. /2/, have extensively examined the theories and procedures for creep determination in isotropic materials, which was the primary emphasis of early investigations. However, many materials are anisotropic. Studies in this area on anisotropic materials were suppressed since it was highly challenging to find solutions in complicated states of stress due to the structure of mathematical models of anisotropy. When anisotropic materials are orthotropic and their anisotropy axes coincide with the primary axes of the cylinder, Bhatnagar et al. /7/ have given simplified models for creep research. Further, the authors explored an orthotropic cylinder experiencing creep under internal and external pressure and came to the conclusion that anisotropic cylinders with greater radial strength survive for a longer period of time. Thakur /16/ used Seth's transition theory to examine creep stresses and strain rates in elastic-plastic materials and came to the conclusion that cylinders with less compressible inner material, and more compressible outer material are more durable than those with the opposite composition. Singh, S.B., et al. /10/ have done extensive study on discs to investigate the creep related stresses and strains under external and internal pressure. Singh, S.B., et al. /10/ had referred to the mathematical modelling related to creep as a threshold stress based creep law. The authors came to the conclusion that FGM discs are superior to homogeneous ones due to better creep response. Further Singh, S.B., et al. /10/ provided a framework for finding stress distribution in anisotropic rotating discs in the presence of residual stress. Singh, S.B. /11/ was able to highlight that aluminium based composite discs having SiC whiskers had significantly different tensile stress distribution due to the residual stress which can significantly limit the service life of component. Singh, T., et al. /13/ investigated transversely isotropic FGM cylinder operating under external and internal pressures. Singh, T., et al. /13/ have also described the creep behaviour of the cylinder by a threshold based creep law. Their study revealed that strain rates decrease significantly when the extent of anisotropy reduces from 1.3 to 0.7.

Numerous studies have been conducted to examine the creep behaviour of composite cylinders, according to the literature review. Only a few research have been done on creep behaviour of anisotropic cylinders. Many of these FGM cylinder investigations make the assumption that the material is isotropic. But practically, all FGMs have an anisotropic character. It must be understood that the majority of materials used in the fabrication of engineering tools and components become anisotropic, so it is crucial that impact of anisotropy is accounted for on engineering components under stress conditions.

ASSUMPTIONS

While performing an analysis of creep, an anisotropic material thick-walled cylinder with internal and external radii of '*a*' and '*b*' respectively is taken into consideration. The pressure inside the cylinder is maintained as a constant '*p*'. The following assumptions are taken into account.

1. Material is anisotropic and incompressible, that is, $\dot{\varepsilon}_r+\dot{\varepsilon}_\theta+\dot{\varepsilon}_z=0$
2. The main axes of the cylinder are same as the anisotropy axes.
3. Creep rate and effective stress are related using Sherby's law, i.e., $\dot{\varepsilon}_e=[M(\sigma_e-\sigma_0)]^n$
4. There is no axial stress, i.e., $\sigma_z = 0$ (plane stress case).

FORMULATION OF CREEP BEHAVIOUR

The constitutive equations given by Bhatnagar et al. /4/ have been used as follows,

$$\dot{\varepsilon}_r=\frac{\dot{\varepsilon}_e}{2\sigma_e}[(G+H)\sigma_r-H\sigma_\theta-G\sigma_z], \quad (1a)$$

$$\dot{\varepsilon}_\theta=\frac{\dot{\varepsilon}_e}{2\sigma_e}[(H+F)\sigma_\theta-F\sigma_z-H\sigma_r], \quad (1b)$$

$$\dot{\varepsilon}_z=\frac{\dot{\varepsilon}_e}{2\sigma_e}[(F+G)\sigma_z-G\sigma_r-F\sigma_\theta]. \quad (1c)$$

Here, $\dot{\varepsilon}_e$ is the creep rate and the effective stress σ_e is defined by the equation

$$\sigma_e=\left[\frac{1}{G+H}\{F(\sigma_\theta-\sigma_z)^2+G(\sigma_z-\sigma_r)^2+H(\sigma_r-\sigma_\theta)^2\}\right]^{\frac{1}{2}}. \quad (2)$$

Using assumption /4/, i.e., $\sigma_z = 0$ in Eqs. (1a), (1b) and (2), one gets

$$\dot{\varepsilon}_r=\frac{du_r}{dr}=\frac{\dot{\varepsilon}_e}{2\sigma_e}[(G+H)\sigma_r-H\sigma_\theta], \quad (3a)$$

$$\dot{\varepsilon}_\theta=\frac{u_r}{r}=\frac{\dot{\varepsilon}_e}{2\sigma_e}[(H+F)\sigma_\theta-H\sigma_r], \quad (3b)$$

$$\sigma_e=\left[\frac{1}{G+H}\{F\sigma_\theta^2+G\sigma_r^2+H(\sigma_r-\sigma_\theta)^2\}\right]^{\frac{1}{2}}. \quad (4)$$

On dividing Eq.(3a) with Eq.(3b) and using $x = \sigma_r/\sigma_\theta$, the resulting equation becomes,

$$\frac{du_r}{dr}\frac{r}{u_r}=\frac{[(G+H)x-H]}{[(H+F)-Hx]}=f(r). \quad (5)$$

Integrating the above Eq.(5) from internal radius '*a*' to *r*,

$$u_r=u_a\exp\left[\int_a^r\frac{f(r)}{r}dr\right]. \quad (6)$$

Here, u_a is radial displacement at internal radius.

On dividing the above Eq.(6) by *r* and equating it with Eq.(3b), one obtains,

$$\frac{u_r}{r}=\frac{\dot{\varepsilon}}{2\sigma_e}[(H+F)\sigma_\theta-H\sigma_r]=\frac{u_a}{r}\exp\left[\int_a^r\frac{f(r)}{r}dr\right]. \quad (7)$$

After applying Sherby's law, the above Eq.(7) becomes,

$$\frac{[M(\sigma_e-\sigma_0)]^n}{2\sigma_e}[(H+F)\sigma_\theta-H\sigma_r]=\frac{u_a}{r}\exp\left[\int_a^r\frac{f(r)}{r}dr\right]. \quad (8)$$

Here, *M*, *n*, and σ_0 are the experimental constant, creep exponent and threshold stress, respectively. Thus,

$$\frac{(\sigma_e-\sigma_0)^n}{\sigma_e}=\frac{2\frac{u_a}{r}\exp\left[\int_a^r\frac{f(r)}{r}dr\right]}{M^n\sigma_\theta[(H+F)-Hx]}. \quad (9)$$

Substituting the value of effective stress from Eq.(4) in Eq.(9), the value of circumferential stress is obtained as,

$$\sigma_\theta=(u_a)^{\frac{1}{n}}g(r)+\sigma_0\frac{\sqrt{G+H}}{\sqrt{(F+H)+(G+H)x^2-2Hx}}, \quad (10)$$

$$g(r)=\frac{1}{M}\left(\frac{2\exp\left[\int_a^r\frac{f(r)}{r}dr\right]}{r[(H+F)-Hx]}\right)^{\frac{1}{n}}\frac{(G+H)^{\frac{n-1}{2n}}}{[(F+H)+(G+H)x^2-2Hx]^{\frac{n-1}{2n}}} \quad (11)$$

According to the equilibrium equation,

$$\frac{d\sigma_r}{dr}=\frac{\sigma_\theta-\sigma_r}{r}\Rightarrow\frac{rd\sigma_r}{dr}+\sigma_r=\sigma_\theta\Rightarrow d(r\sigma_r)=\sigma_\theta dr. \quad (12)$$

Integrating Eq.(12) from internal to external radius and using boundary conditions (at internal radius $r = a$, $\sigma_r = -p$, and at external radius $r = b$, $\sigma_r = 0$, it becomes

$$[r\sigma_r]_a^b=\int_a^b\sigma_\theta dr\Rightarrow ap=\int_a^b\sigma_\theta dr. \quad (13)$$

Using the value of tangential stress given by Eq.(10) in Eq.(13) and calculating the value of $(u_a)^{1/n}$ from the expression, one gets

$$\frac{ap-\sigma_0\sqrt{G+H}\int_a^b\frac{1}{\sqrt{(F+H)+(G+H)x^2-2Hx}}dr}{\int_a^b g(r)dr}=(u_a)^{\frac{1}{n}}.$$

Substituting the above value in Eq.(10),

$$\sigma_\theta=\frac{ap-\sigma_0\sqrt{G+H}\int_a^b\frac{1}{h(r)}dr}{\int_a^b g(r)dr}g(r)+\sigma_0\frac{\sqrt{G+H}}{h(r)},$$

taking $h(r)=\sqrt{(F+H)+(G+H)x^2-2Hx}$. (14)

Again integrating the equilibrium equation from *a* to *r*, one gets

$$\sigma_r=\frac{1}{r}\int_a^r\sigma_\theta dr-\frac{ap}{r}. \quad (15)$$

MATHEMATICAL CALCULATIONS

The following data has been taken from Singh, T., et al. /13/ and Bhatnagar et al. /5/.

The values of *F*, *G*, and *H* have been taken as follows

Case 1: $F = 1$, $G = 0.5$, and $H = 1.5$

Case 2: $F = 1$, $G = 1$, and $H = 1$ (isotropic case)

Case 3: $F = 1$, $G = 0.75$, and $H = 1.25$

Cylinder is made up of aluminium silicon carbide particulate (Al-SiC_p) composite with $P = 1.7$ µm, $T = 450$ °C, $V =$

20 vol.%SiC$_p$, p = 85.25 MPa, M = 5.92×10^{-3} s$^{-1/5}$ per MPa, σ_0 = 29.18 MPa, n = 5.

The cylinder is assumed to have a = 1, and outer radius b = 2 for the analysis of results.

To find the first approximation of x, tangential stress is assumed to be uniform and equal to $\sigma_{\theta\, average}$.

Using $\sigma_\theta = \sigma_{\theta\, average}$ in Eq.(15) of σ_r and $ap = \int_a^b \sigma_\theta dr$, one gets

$$\sigma_r = \frac{\sigma_{\theta\, average}}{r}(r-a) - \frac{ap}{r} \quad \text{and} \quad \sigma_{\theta\, average} = \frac{ap}{b-a},$$

thus,
$$\frac{\sigma_r}{\sigma_{\theta\, average}} = 1 - \frac{b}{r} = (x)_1. \qquad (16)$$

Equation (16) is the first approximation of x.

The integrals of σ_θ and σ_r have been calculated using the iterative techniques as per the following methodology.

For obtaining new values of x, the following methodology is deployed till the time the old value of x becomes equal to, or becomes nearly equal to the new value of x, i.e., up to four decimal positions:

1. Initial values of x are calculated using Eq.(16) for different values of radius.
2. Calculate the values of $f(r)$ using Eq.(5).
3. Calculate values of $\int_a^r \frac{f(r)}{r} dr$ using numerical integration.
4. Calculate different values of $g(r)$ as in Eq.(11), at various radii using the above.
5. Calculate values of $\int_a^b g(r)dr$ and $\int_a^b \frac{1}{h(r)} dr$ using numerical integration.
6. Calculate values of σ_θ using the above values in Eq.(14).
7. Calculate σ_r using the above value in Eq.(15).
8. New value of σ_r is calculated using Eq.(16).
9. The procedure is repeated again and again, until the new values of x become equal to the old values of x.
10. Iteration is stopped when the difference between two values of x in subsequent iterations become zero or the errors are limited to four decimal positions.

The calculated values of tangential and radial stress are shown in Table 1 for some values of r. The calculated values of effective stress and creep rate are shown in Table 2 for some values of r.

Table 1. Tangential and radial stress values at different values of radii.

	Tangential stress (MPa)			Radial stress (MPa)		
r	Case 1	Case 2	Case 3	Case 1	Case 2	Case 3
1.0	59.2142	57.5929	58.5007	-85.2500	-85.2500	-85.2500
1.1	67.0059	66.2919	66.6929	-71.7627	-71.8689	-71.8094
1.2	73.5388	73.4643	73.5054	-59.9265	-60.0566	-59.9837
1.3	79.0586	79.3856	79.2004	-49.4476	-49.5580	-49.4962
1.4	83.7535	84.2832	83.9843	-40.1009	-40.1729	-40.1328
1.5	87.7703	88.3412	88.0198	-31.7101	-31.7405	-31.7238
1.6	91.2242	91.7076	91.4365	-24.1346	-24.1302	-24.1330
1.7	94.2070	94.5020	94.3377	-17.2611	-17.2340	-17.2495
1.8	96.7927	96.8206	96.8069	-10.9966	-10.9621	-10.9816
1.9	99.0412	98.7420	98.9118	-5.2643	-5.2387	-5.2532
2.0	101.0016	100.3302	100.7080	0.0000	0.0000	0.0000

Table 1 gives the values of tangential and radial stress. Table 2 gives the values of effective stress and creep rate based on different values of F, G, and H. These values have been calculated using Eqs. (14), (15), (4), and Sherby's law respectively, at various values of radii.

Table 2. Effective stress and creep rate at different values of radii.

	Effective stress (MPa)			Creep rate		
r	Case 1	Case 2	Case 3	Case 1	Case 2	Case 3
1.0	138.6452	124.4761	131.7258	0.11428	0.05715	0.08245
1.1	134.0705	119.6833	127.0708	0.09232	0.04415	0.06536
1.2	130.2364	115.8266	123.2391	0.07664	0.03551	0.05353
1.3	126.9715	112.6600	120.0284	0.06503	0.02948	0.04500
1.4	124.1543	110.0155	117.2980	0.05619	0.02510	0.03863
1.5	121.6957	107.7758	114.9466	0.04928	0.02181	0.03374
1.6	119.5294	105.8560	112.9000	0.04378	0.01927	0.02991
1.7	117.6045	104.1935	111.1022	0.03931	0.01727	0.02683
1.8	115.8816	102.7412	109.5102	0.03562	0.01566	0.02432
1.9	114.3295	101.4629	108.0906	0.03255	0.01435	0.02225
2.0	112.9232	100.3302	106.8170	0.02995	0.01326	0.02051

GRAPHICAL REPRESENTATION OF THE RESULTS

After plotting their scattered plots using Tables 1 and 2, it is clear that radial stresses are approximately similar for all three cases, one of isotropy and two of anisotropy. The curves of radial stresses represented in Fig. 1, overlapped. The curves show that the radial stress varies from pressure value at inner radius to the pressure value at outer radius, such that the radial stress reduces faster initially than at a later stage in the radial direction from inner to outer radius.

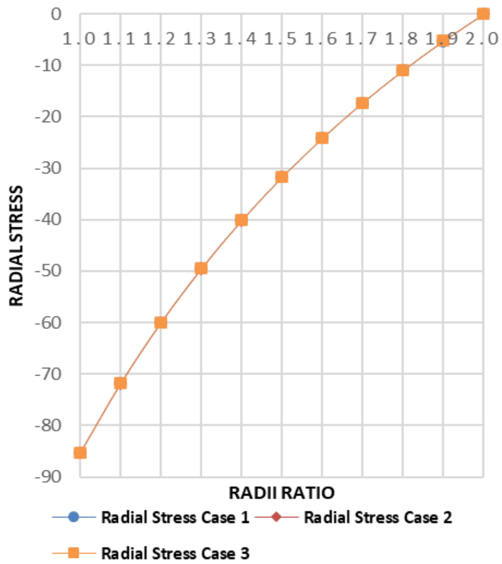

Figure 1. Radial stress vs. r/a.

Similarly, barring minute differences in the values of tangential stress in the three cases, one of isotropy and two of anisotropy, the curves of tangential stresses represented in Fig. 2 nearly overlap. In this case also, the tangential stress curve increases as the radius increases but are in the range between 57 to 101 MPa. Here also the slope of the curve reduces in radial direction from inner to outer radius.

A noticeable difference in the values of effective stress is observed in all three different cases in Fig. 3. It is observed that in plane stress conditions, the effective stress is minimal in the isotropic case as against that experienced in the anisotropic cases, under similar conditions. Further, it is noted that the effective stress reduces along the radius from inner to outer direction.

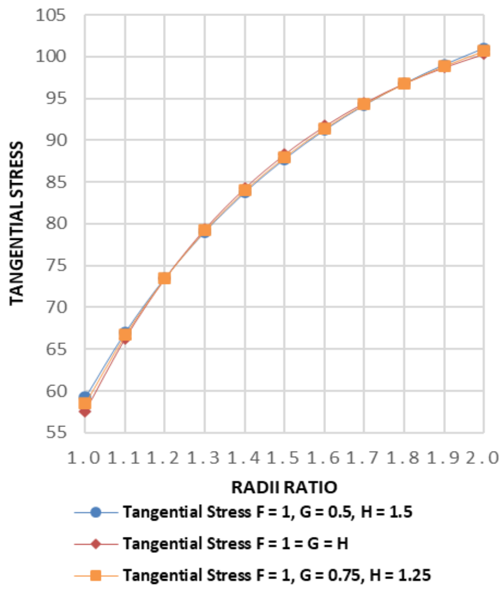

Figure 2. Tangential stress vs. *r/a*.

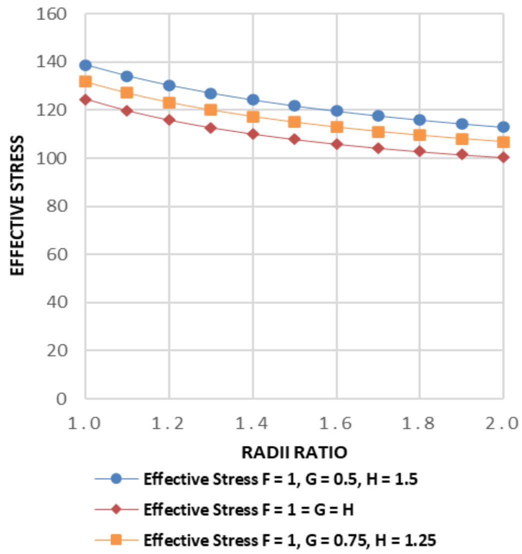

Figure 3. Effective stress vs. *r/a*.

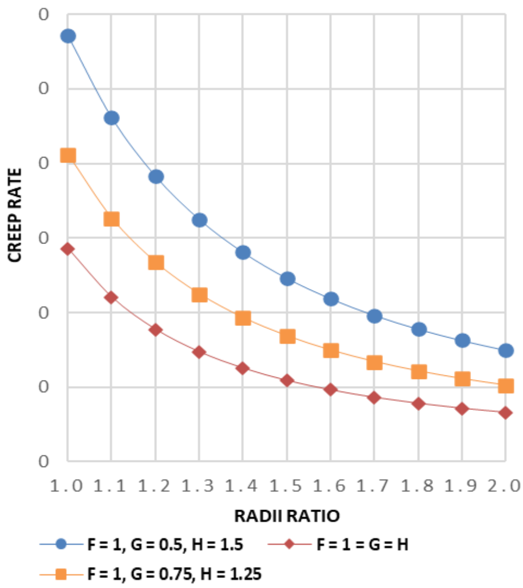

Figure 4. Creep rate vs. *r/a*.

Figure 4 represents the creep rate decreases along the radius in plane stress condition, having only internal pressure. Here, also it may be seen that in plane stress conditions, creep rate is lower in isotropic cases as against the anisotropic cases. Which means that isotropic materials behave better than anisotropic materials in such plane stress conditions.

Figure 5 depicts effective stress versus creep rate in all the three cases, one isotropic and two anisotropic cases. The creep rate is found to increase with increase in effective stress.

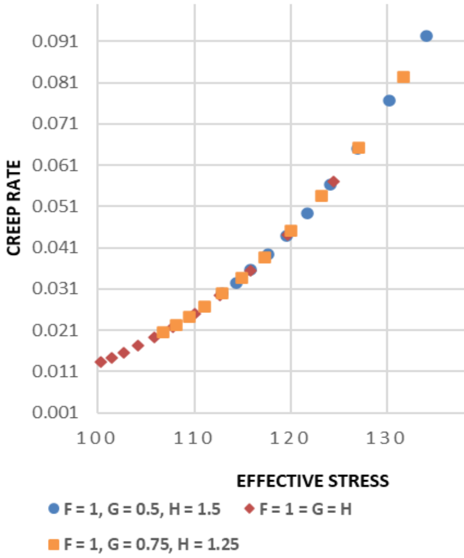

Figure 5. Effective stress vs. creep rate.

DISCUSSION AND CONCLUSION

Material anisotropy is found to significantly impact the creep behaviour of thick-walled cylinders. Bhatnagar et al. /6/ had found that anisotropy reduces stresses in the cylinder and thus makes them safer from design consideration. However, the authors find that effect of anisotropy is relatively small on the stress distribution. Singh, T. et al. /13/ confirmed the finding that anisotropy induces significant strain rate changes, although its effect on the resulting stress distribution is relatively small. In their study, the authors also establish that anisotropy helps in restraining creep responses both in tangential and radial directions.

The effect of anisotropy on a thick-walled cylinder under constant internal pressure in plane stress condition reveals that radial and tangential stress distribution hardly varies along the radius of the cylinder with change in anisotropic parameters. But in plane stress condition, the effective stress and creep response is found to be smaller in the case of isotropic materials than in anisotropic ones.

Whereas, in general, anisotropy helps in reducing the stresses and strain in thick-walled cylinders in plane stress condition. Isotropic materials are found to be better from the engineering design point of view, as isotropic material exhibits lesser effective stress and creep response.

REFERENCES

1. Badini, C. (1990), *SiC whiskers-aluminium 6061 composite: microstructure and mechanical characteristic anisotropy*, J Mater. Sci. 25: 2607-2614. doi: 10.1007/BF00638066
2. Rimrott, F.P.J., Luke, J.R. (1961), *Large strain creep of rotating cylinders*, J Appl. Math. Mech. 41(12): 485-500. doi: 10.1002/zamm.19610411203
3. Mishra, R.S., Pandey, A.B. (1990), *Some observations on the high-temperature creep behavior of 6061 Al-SiC composites*, Metall. Trans. A, 21: 2089-2090. doi: 10.1007/BF02647258
4. Bhatnagar, N.S., Gupta, R.P. (1966), *On the constitutive equations of the orthotropic theory of creep*, J Phys. Soc. Japan, 21 (5): 1003-1007. doi: 10.1143/JPSJ.21.1003
5. Bhatnagar, N.S., Gupta, S.K. (1969), *Analysis of thick-walled orthotropic cylinder in the theory of creep*, J Phys. Soc. Japan, 27(6): 1655-1661. doi: 10.1143/JPSJ.27.1655
6. Bhatnagar, N.S., Arya, V.K. (1974), *Large strain creep analysis of thick-walled cylinders*, Int. J Non-Linear Mech. 9(2): 127-140. doi: 10.1016/0020-7462(74)90004-3
7. Bhatnagar, N.S., Kulkarni, P.S., Arya, V.K. (1986), *Creep analysis of orthotropic rotating cylinders considering finite strains*, Int. J Non-Linear Mech. 21(1): 61-71. doi: 10.1016/0020-7462(86)90013-2
8. Pandey, A.B., Mishra, R.S., Mahajan, Y.R. (1992), *Steady state creep behaviour of silicon carbide particulate reinforced aluminium composites*, Acta Metallurgica et Materialia, 40(8): 2045-2052. doi: 10.1016/0956-7151(92)90190-p
9. Hill, R. (1948), *A theory of the yielding and plastic flow of anisotropic metals*, Proc. Royal Soc. A: Math. Phys. Eng. Sci. 193 (1033): 281-297. doi: 10.1098/rspa.1948.0045
10. Singh, S.B., Ray, S. (2002), *Modeling the anisotropy and creep in orthotropic aluminum-silicon carbide composite rotating disc*, Mech. Mater. 34(6): 363-372. doi: 10.1016/S0167-6636(02)00132-1
11. Singh, S.B. (2008), *One parameter model for creep in a whisker reinforced anisotropic rotating disc of Al-SiC$_w$ composite*, Eur. J Mech. A/Solids, 27(4): 680-690. doi: 10.1016/j.euromechsol.2007.11.004
12. Bansal, S., Singh, S.B. (2022), *Creep analysis of thick walled cylinder under constant pressure*, Mater. Sci. Forum, 1074: 89-106. doi: 10.4028/p-904ahp
13. Singh, T., Gupta, V.K. (2009), *Effect of material parameters on steady state creep in a thick composite cylinder subjected to internal pressure*, J Eng. Res. 6(2): 20-32. doi: 10.24200/tjer.vol6iss2pp20-32
14. Arya, V.K., Bhatnagar, N.S. (1976), *Creep of thick-walled orthotropic cylinders subject to combined internal and external pressures*, J Mech. Eng. Sci. 18(1): 1-5. doi: 10.1243/jmes_jour_1976_018_003_02
15. Wahl, A.M., Sankey, G.O., Manjoine, M.J., Shoemaker, E. (1954), *Creep tests of rotating disks at elevated temperature and comparison with theory*, J Appl. Mech. 21(3): 225-235. doi: 10.1115/1.4010898
16. Gupta, S.K., Thakur, P. (2007), *Creep transition in a thin rotating disc with rigid inclusion*, Def. Sci. J, 57(2): 185-195. doi: 10.14429/DSJ.57.1745